HHS Public Access

Author manuscript

Semin Ultrasound CT MR. Author manuscript; available in PMC 2016 June 01.

Published in final edited form as:

Semin Ultrasound CT MR. 2015 June ; 36(3): 234–248. doi:10.1053/j.sult.2015.05.015.

Imaging of the Functional and Dysfunctional Visual System

Edgar A. DeYoe, PhD[*], **John L. Ulmer, MD**[*], **Wade M. Mueller, MD**[†], **David S. Sabsevitz, PhD**[‡], **Danielle C. Reitsma, PhD**[*], and **Jay J. Pillai, MD**[§]

[*]Department of Radiology, Medical College of Wisconsin, Milwaukee, WI

[†]Department of Neurosurgery, Medical College of Wisconsin, Milwaukee, WI

[‡]Department of Neurology, Medical College of Wisconsin, Milwaukee, WI

[§]Department of Radiology, Johns Hopkins University, Baltimore, MD

Abstract

Functional magnetic resonance imaging (fMRI) is used clinically to map the visual cortex before brain surgery or other invasive treatments to achieve an optimal balance between therapeutic effect and the avoidance of postoperative vision deficits. Clinically optimized stimuli, analyses, and displays permit identification of cortical subregions supporting high-acuity central vision that are critical for reading and other essential visual functions. A novel data display permits instant appreciation of the functional relationship between the pattern of fMRI brain activation and the pattern of vision loss and preservation within the patient's field of view. Neurovascular uncoupling and its detection in the visual cortex are key issues for the interpretation of fMRI results in patients with existing brain pathology.

Introduction

Human visual perception arises from a sensory system that includes the eyes with their photoreceptors and retinal neurons, subdivisions of the thalamus, numerous subdivisions of the cerebral cortex within the occipital lobe, and adjacent portions of the temporal and parietal lobes plus a myriad of cortical and subcortical pathways that interconnect these various regions. Functional specialization within this system, especially within the different subdivisions of the visual cortex, supports a variety of specific visual abilities including the perception of form, color, texture, motion, stereopsis, faces, places, and higher-order metaproperties such as objectness; the organization of 3-dimensional (3D) space; the perception of complex motion sequences (eg, dance); and critical visual abilities such as reading. Although the association of different perceptual attributes with different neuronal subsystems is appreciated at a coarse level, it is a common misconception that individual perceptual properties arise exclusively from individual cortical subdivisions such as a “color area,” “motion area,” or “word-form area.” Although it is true that discrete lesions of restricted portions of the visual cortex can produce somewhat selective deficits such as prosopagnosia, achromatopsia, or akinetopsia, this merely indicates that the associated

Address reprint requests to Edgar A. DeYoe, Medical College of Wisconsin, Department of Radiology, 8701 Watertown Plank Rd, Milwaukee, WI 53226. deyoe@mcw.edu, jayamparibala@gmail.com.

lesion has intersected a critical nexus of a multielement subsystem extending from the retina to the highest levels of the cortex. Moreover, components of a functional subsystem at one hierarchical level may be shared with other subsystems, which then diverge and reconverge at other levels of the hierarchy. Concurrently, higher levels of processing modulate earlier levels of processing via feed-back connections that reciprocate virtually every feed-forward connection, thereby providing for both bottom-up and top-down influences on visual processing. The top-down effects provide active selection of locations and features that may become the focus of subsequent detailed visual analysis through eye movements and shifts of attention, all operating dynamically as a task or behavior evolves over time.

The relevance of this seemingly daunting complexity for clinical science is yet to be fully appreciated. Understanding such complexity may hold the key to developing a more sophisticated and powerful understanding of the relationships between brain damage and vision deficits and may suggest rehabilitative strategies or compensatory behaviors to assist patients with brain-related vision deficits. Our current ability to account for an individual patient's vision symptomatology through association with specific sites of damage and specific neuropathologic processes is good. But we have yet to fully incorporate the most recent research advances and integrate them with our increasing ability to identify and map the structure and function of visual pathways in individual patients. The focus of this article, then, is mainly to highlight the structure and function of the human visual system, as revealed by medical imaging technology, particularly magnetic resonance imaging (MRI), which is increasingly available to clinicians. We also review clinical case reports that illustrate how imaging the visual system of individual patients having focal pathologies can assist diagnosis and guide treatment. Though patients having brain-related vision deficits may be less common than patients having, say, language or movement deficits, they still deserve the best, most sophisticated care that clinical science can provide. A requisite step along the path to improved treatment and outcomes is a more sophisticated appreciation of the increasingly detailed information and diagnostic techniques enabled by modern imaging technology.

Visual Cortex Functional Anatomy

Functional mapping of the human visual system using modern imaging technologies has been a focus of several previous reviews that should be consulted for technical details concerning imaging methodologies and paradigms.[1–5] Figure 1 illustrates an approximate anatomical layout of occipital visual areas in human neocortex displayed as 3D cortical surface maps (right) and as a cortical “flat map” (left) to allow better appreciation of the overall topography. For clinical utility, the 3D rendition is often more readily matched to the patient's intact anatomy and to conventional slice-based anatomical images.

The structural and functional connectivity of these various visual areas in humans is currently the focus of significant ongoing effort, most notably associated with the National Institutes of Health-funded Human Connectome Project and other major efforts.[6,7] However, at this juncture, the most extensive and reliable account of visual system connectivity comes from nonhuman primates, notably macaque monkeys, whose visual abilities appear to rival those of humans. Figure 2 illustrates the connectivity of analogous or

homologous visual areas in the macaque monkey (gray underlay) and provides a potential template for the human visual connectome, albeit with undoubted modifications to be added, as relevant, reliable human data become available in the near future. The complexity of the macaque visual connectome far exceeds our current ability to understand its clinical relevance in any detailed fashion. Yet, it can suggest potential clinical interpretations or "scenarios" where previously none or only crude estimates may have existed. For example, the macaque middle temporal visual area, whose homolog is thought to be part of the human TO complex (Fig. 2), is characterized by neurons that respond selectively to the direction and speed of a moving visual stimulus. Referencing such properties, Zeki reported a case study of a woman having bilateral cortical lesions that rendered her unable to accurately perceive the motion of objects in her visual world.[8] Zeki[8] proposed that the patient's deficit, akinetopsia, might logically arise from damage to the human equivalent of the macaque middle temporal visual area. In a similar vein, Zeki[9] proposed that cerebral achromatopsia might arise from selective damage of a distinct visual area in the ventral occipital-temporal cortex (V4) that possessed neurons that responded selectively to visual stimuli varying in color.

Zeki's perspective has become increasingly relevant as more distinct visual areas have come to light and as injectable anatomical "tracers" have made it possible to chart the patterns of axonal projections interconnecting pairs of visual areas.[10–13] In turn, this has led to a growing appreciation of functionally distinct brain networks and their associated gray and white matter components. In this respect, a seminal insight was proposed by Ungerleider et al,[14] who proposed that the corticocoitical visual pathways could be roughly separated into ventral vs dorsal "processing streams" that, when damaged, were associated with distinct patterns of visual dysfunction. Ventral damage typically disrupted the ability to identify or discriminate objects differing in shape or pattern, whereas dorsal stream lesions disrupted "landmark" tasks requiring use of spatial proximity information. Such results led to the proposal that the cortical visual system is organized as a ventral "what" pathway vs a dorsal "where" pathway.[14] Though crude and subsequently modified,[15] these clinically relevant insights arguably arose from consideration of the (then) newly discovered array of distinct visual areas and the burgeoning elucidation of their connectivity. Today as we extend these early efforts to human patients through modern neuroimaging technology, the seemingly daunting complexity of the resulting data (eg, Figs. 1 and 2) will begin to yield new insights as clinician-scientists seek increasingly detailed and specific explanations for the clinical manifestations that they encounter in their patients.

To add a more functional perspective to the anatomical and connectional diagrams of Figures 1 and 2, the Table provides a summary of some of the perceptual contributions of different cortical visual areas and subnetworks to which they belong. Some areas in the Table are not included in the diagram of Figure 1 (eg, frontal areas), and some areas listed in the Table (fusiform face area and word-form area) may overlap or extend (parahippocampal place area) portions of VO-1–2 in Figure 1. This uncertainty in part reflects different criteria and terminology used by different authors to define these areas. Early cortical visual areas (V1, V2, and V3) appear to be involved in a variety of low-level processing tasks that then feed multiple parallel processing networks ascending into the parietal and temporal cortices. Consistent with the notion of distinct dorsal and ventral processing "streams," the dorsal

stream visual areas are heavily involved in the processing of different types of motion and associated movements of the eyes and body relative to end-point targets. In contrast, ventral visual areas are heavily involved with the analysis of visual features such as form, color, textures, and higher-order configurations such as faces, all of which contribute to the recognition and identification of objects. As the different processing streams physically spread out from posterior occipital areas, they become selectively vulnerable to focally restricted damage that can then result in selective visual agnosias rather than scotomata (local zones of blindness). Several of these agnosias including prosopagnosia (faces), achromatopsia (colors), and akinetopsia (movement) have been associated with lesions of specific visual areas, as noted in the Table, though often such deficits are not exclusively associated with just those areas. In sum, Figures 1 and 2 and the Table provide a conceptual basis for beginning to understand the detailed relationships between cortical damage and specific visual symptoms observed in individual patients. This is increasingly aided by the ability to obtain patient-specific clinical tests and neuroimaging data, as outlined in the next section.

fMRI Vision Mapping Methods

A particularly informative and efficient method for functional magnetic resonance imaging (fMRI) mapping of the human visual cortex is to use stimuli consisting of slowly expanding checkered annuli and slowly rotating checkered pie wedges typically extending out to an eccentricity of 20°-25° from the center of gaze (Fig. 3, left). (For additional methodological details see Gill et al[53] and DeYoe et al.[4]) The checkerboard patterns are composed of high contrast, black-and-white checks that counterphase flicker at 8 Hz, resulting in strong neural activation and relatively large increases in the blood oxygen level-dependent (BOLD) fMRI signal. Both visual field eccentricity (Fig. 3, upper row) and angular position (Fig. 3, lower row) can be mapped in this manner using fMRI scans of approximately 4–6 minutes duration. When combined with anatomical MRI scans, the whole study can be accomplished in as little as 30 minutes.

The resulting data are then subjected to a temporal phase analysis in which the timing of the fMRI response is used to identify the location in the patient's visual field that, when stimulated, most strongly activates each responsive brain voxel. The resulting cortical maps not only delineate visual cortex but also can identify subzones supporting vision at the center of gaze, which is critical for reading and many daily activities. The resulting maps also can be used to identify multiple, functionally distinct, visual areas (as illustrated in Figure 1) and can be used to construct functional field maps (FFMaps), as illustrated at the right of Figure 3.

FFMaps are composed of circle symbols, each of which corresponds to a visually responsive voxel in the visual cortex that was maximally activated by stimuli presented at the location of the symbol within the visual field. The color of each circle indicates the strength of the fMRI response, whereas the size represents an estimate of the error in measuring the preferred stimulus position. For a healthy individual, the FFMap would contain circle symbols distributed throughout the visual field. But, if the visual cortex is focally damaged, symbols would be missing or reduced in number within the retinotopic zone of the visual

field affected by the pathology (illustrated in the FFMap of Figure 3 by the hatched area). Thus, the FFMap provides a unique display that can instantly reveal the relationship between a cortical pattern of focal pathology and its effects on the patient's field of vision.

Clinical Applications

Clinically, fMRI vision mapping has been used for presurgical planning and surgical guidance for patients with pathology or potential surgical involvement of the central visual pathways.[1,4,53,54] Studies comparing fMRI and intraoperative cortical stimulation in the visual cortex have reported good correspondence.[55,56] When a resection is necessary, neurosurgeons are able to use knowledge gained from the fMRI maps to help plan an optimal approach and extent of resection that maximizes therapeutic value yet avoids damage to neighboring eloquent cortex that may be critical for daily visual function. Detailed mapping of the visual cortex in combination with diffusion tensor imaging to identify specific white matter tracts such as the optic radiations can provide complementary information and a more complete picture for presurgical planning. Using this information in conjunction with a detailed surgical plan can help identify and evaluate the potential for treatment-induced vision loss. This may be particularly important for pathologies associated with long-term survival for which preserved visual function may be essential to maintain the patient’s quality of life for as long as possible.

The following case reports provide illustrative examples of patients and conditions for which vision mapping was found to be clinically useful. In all instances, fMRI mapping was included as part of a comprehensive workup to identify and delineate the pathology, map neighboring eloquent cortex, and delineate critical white matter tracts that might be at risk. In this context, it is important to note that fMRI mapping typically does not replace existing methods such as intraoperative electrocortical stimulation but, rather, extends and clarifies these more conventional tests and interpretations. In some cases, fMRI may simply verify that a treatment plan motivated by other considerations is likely to be benign concerning induced vision deficits.

Illustrative Case Reports

Occipitotemporal Tumor

Figure 4A illustrates vision fMRI results for a 65-year-old male patient with an occipital tumor plus edema of the left, ventral, temporal lobe extending posteriorly into the occipital lobe. The patient complained of difficulty reading words and comprehending written information. Behavioral visual field testing revealed normal visual sensitivity in the left hemifield but significantly reduced sensitivity throughout much of the right visual field, especially in the upper right periphery (Fig. 4C, dark squares in background perimetry chart). A potential plan to aggressively resect the tumor was being considered, as its location appeared likely to have destroyed the optic radiations, thereby “disconnecting” the left occipital visual cortex from its retinal input. Surprisingly, vision fMRI revealed a largely normal pattern of activation in the right hemisphere within medial and posterior portions of the occipital lobe on the side of the lesion (Fig. 4A). Moreover, diffusion tensor imaging tractography, illustrated in Figure 4B, revealed that the optic radiations had not been

destroyed but had been displaced dorsally (white dotted line) by the tumor, leaving them capable of driving the visual activation evident in the fMR images.

To compare the fMRI pattern with the behavioral perimetry more precisely, an FFMap was constructed from the vision mapping data and was superimposed on the patient's perimetry chart for the central 20° of eccentricity (Fig. 4C). Consistent with the zone of dense vision loss in the upper right periphery of the perimetry chart (underlay, black squares), there were fewer voxels (circle symbols) associated with the far right peripheral field. Closer to the vertical midline, however, visually responsive voxels (circle symbols) appeared at roughly normal density despite impaired vision in this region. This suggested that the vision deficit was not solely due to lack of sensory input. Perhaps careful debulking of the tumor could relieve pressure or other pathologic effects on the adjacent optic radiations and gray matter, allowing some recovery of visual function. Other functionally critical regions such as the visual word-form area [50,57,58] and temporal language areas (Fig. 4B, red arrow) abutted the tumor laterally and anteriorly, posing additional constraints on the surgical plan.

Surgery was performed with the patient alert, thereby permitting detailed intraoperative testing of vision and language functions. This was aided by use of an ultrasonic aspirator that tends to “stun” but not destroy brain tissue in a penumbra surrounding the tip. Proximity of the aspirator to the presumed visual word-form area antromedial to the tumor caused transient reading difficulties, thus limiting the anterior extent of resection. Laterally, the resection was limited by transient impairment of language comprehension. Posteriorly, the surgery avoided visually responsive gray matter and the optic radiations dorsally. Ultimately, the resection was successful in removing much of the tumor mass, and the patient recovered with improved reading and language comprehension.

Virtual Surgery

Figure 5 illustrates data from an epileptic patient with an apparent occipital lobe seizure focus indicated by electro-encephalographic monitoring. The seizure focus was roughly mapped to the right occipital pole, which on careful examination of the T1-weighted anatomy (Fig. 5A) revealed subtle thinning of the occipital gray matter. Resection of the occipital pole was considered a possible treatment option, but the location and extent of potential vision loss was an important consideration. To help provide an estimate of the potential loss, fMRI vision mapping was performed. As shown in Figure 5A, visually driven activation was observed throughout the occipital lobe, most notably within the right medial and posterior pole, encompassing the planned resection zone (white outline). A unique color code was used to identify the visual field eccentricity represented by each visually active voxel with red and yellow representing the critical foveal representation, as indicated by the inset in Figure 5A. This clearly indicated that the planned resection would affect vision near the center of gaze. To provide even more information, an FFMap (Fig. 5B) was constructed for this patient using both fMRI rings and rotating wedge data (wedge data not shown). This allows identification of the specific location within the patient's visual field that is represented by each active voxel (the location at which the voxel was maximally activated by the ring and wedge stimuli). A 3D region of interest (ROI) encompassing the complete planned resection volume was outlined on all relevant sections of the T1-weighted images.

(Fig. 5A, white outline shows only the ROI within the illustrated section. The complete ROI extended several sections above and below.) The ROI was then used to identify visually responsive brain voxels that would be destroyed by the planned resection. The corresponding symbols in the FFMap of Figure 5B were removed to yield the representation in Figure 5C. This "virtual surgery" thus provided an estimate of the region of the patient's visual field that would be affected by the resection (white dashed outline in Figure 5C). Comparing Figure 5B and C reveals that the most significant loss of brain activity (reduced number of circle symbols) would be in the lower left quadrant extending into the perifoveal region of the upper quadrant. During reading, vision loss in the left visual field can potentially disrupt the targeting of "return" saccades that occur when the reader completes reading a line of text and makes a leftward eye movement back to the beginning of the next line.[59,60] Smooth effortless reading might thus be disrupted, which could significantly affect the patient's ability to perform a job if it required large amounts of reading. As of this writing, the patient had not undergone surgery and seizures were being managed pharmacologically as much as possible.

Epilepsy With Gray Matter Heterotopia

Figure 6 illustrates multiparametric imaging data for an epileptic patient with potential initiating foci near the temporal-parietal-occipital junction and the angular gyrus. FMRI visual field mapping produced robust activation throughout the occipital visual cortex (Fig. 6B, yellow-orange voxels). Examination of T1-weighted anatomical images revealed gray matter heterotopia in the right occipitotemporal region, as highlighted by the white arrow in Figure 6A. However, a diffusion tensor imaging orientation map (white matter coloring in 6B) showed that the heterotopia was positioned within the optic radiations (green tract with white arrow). Potential resection of the heterotopia would likely disrupt the retinal input that is driving the visual cortex activation in that same hemisphere. Consequently, at surgery, the highlighted heterotopia was not targeted for resection. Instead, an anterior temporal lobectomy was performed along with additional focal topectomies in the parietal and the temporal lobes based on implanted electrode grid recordings. The patient recovered well and is largely seizure free.

Aberrant Cortical Organization and the Potential for Reorganization

A recurring question when working with patients having central visual system pathology is "can the visual system reorganize," thus providing some hope for recovery of lost visual function. Classically, the answer, has been "no, not significantly."[61] However, there is accumulating evidence that some plasticity can occur with rehabilitation training [61,62] and that aberrant retinotopic organization can occur in some rare congenital and late-onset pathologies.[63] Recently, Reitsma et al[63] examined 27 patients for indications of unusual cortical retinotopic organization. These patients had a variety of central visual system pathologies including stroke, tumors, arteriovenous malformations (AVM), congenital malformations, and surgical resections. Figure 7A shows FFMaps for a patient who had congenital hydrocephalus. Each FFMap was constructed from a single hemisphere, as depicted by the white dotted line in the underlying axial fMR image. The FFMap for the right visual field (left hemisphere) appeared to have a relatively normal hemifield representation. However, the FFMap for the left visual field (right hemisphere) was aberrant

in having a large number of voxels representing locations in the ipsilateral visual field (surrounded by the white dashed outline in the FFMap). The lower panel of Figure 7 provides a more quantitative view of this aberrant organization. Each point on the perimeter of the yellow shaded area shows the number of voxels representing each angular meridian of an average, healthy subject's visual field. For example, there were approximately 22 voxels (between 16 and 24) representing a thin sector along the left horizontal meridian. It should be noted that for healthy individuals, very few voxels represent meridia in the ipsilateral visual field (to the right of the vertical meridian). However, the voxel distribution for the aforementioned patient with hydrocephalus was markedly different, as illustrated by the red shaded area that extends well into the ipsilateral (right) visual field. Of the sample of 27 patients, 3 showed such an expanded representation of the ipsilateral visual field that was up to 3 times larger than that of healthy subjects. Though rare, such cases do prove that under certain pathologic conditions, cortical organization can change in adults; however, it is unclear whether this represents true reorganization or unmasking of normally “subthreshold” organizational features. It is also not clear if such unusual organization necessarily imparts expanded visual capabilities, though in 1 patient of the Reitsma study, the expanded ipsilateral field representation appeared to be associated with a strip of preserved visual sensitivity in the ipsilateral field of the patient's perimetry chart. However, this rare case must be interpreted with caution, as there was no verification that the patient was using the central fovea to fixate the center of the perimetry display during testing. In the Reitsma study, the authors speculate that the expanded representation of the ipsilateral field near the vertical meridian may be “unmasked” because of the loss of normally suppressive inputs from damage to the contralateral hemisphere. Whether it is possible for such effects to occur under other conditions and for other parts of the visual field remains unclear.

More dramatic aberrations in cortical retinotopic organization are known to occur in association with peripheral visual system pathologies such as albinism and achiasma.[64–71] Illustrated in Figure 8C–F are cortical retinotopic maps for an albinistic patient obtained under monocular, right eye, viewing conditions in which each hemifield was mapped separately using a half ring stimulus, as depicted schematically in the diagrams at the lower left. As might be expected, the ring sequence in the right hemifield produced a normal eccentricity mapping of the central visual field in the visual cortex of the contralateral (left) occipital lobe (Fig. 8C, inset shows color code). However, surprisingly, the ring sequence in the left hemifield produced a nearly identical map in the left occipital lobe (Fig. 8E). This is a very aberrant mapping, because, in nonalbinistic subjects, the left visual field normally projects to the right occipital lobe, not the left. The reverse was largely the case for this patient, except for the peripheral field and for some extrastriate visual areas in the ventral lateral cortex. Functionally, one might expect that this aberrant cortical organization would be a problem, as opposite halves of the visual field project to, and are superimposed within, the same (left) hemisphere. Consequently, the same location in the visual cortex is activated by stimuli at completely separate (mirrored) locations in space. How the visual cortex neurons sort out the conflicting visual inputs and why such albinistic patients do not have completely aberrant visual sensations is not entirely clear, though at least 2 different theories have been advanced to explain this.[72] The important point in the present context is that

fMRI visual field mapping can reveal grossly aberrant features of brain organization that may not be readily apparent from simple, conventional clinical tests.

A Cautionary Note: Neurovascular Uncoupling

fMRI maps provide an indirect measure of brain activity because the BOLD response reflects a cascade of cellular and chemical events that link neural activity to local changes in cerebral blood flow, blood volume, and blood oxygenation.[73–75] Ultimately, these latter factors alter the relative volume of oxygenated to deoxygenated hemoglobin contained in each imaging voxel. When neuronal activity within a voxel increases, the vasculature dilates, causing an influx of freshly oxygenated hemoglobin and a decrease in the proportion of deoxyhemoglobin. This reduces the magnetic field heterogeneity in the voxel (because of the presence of deoxyhemoglobin) that, in turn, allows water protons to emit a stronger, more coherent signal. However, under certain circumstances, focal brain pathology can disrupt this hemodynamic mechanism, yet leave the underlying neural activity more or less intact—a phenomenon known as neurovascular uncoupling (NVU). NVU can arise from a disruption at any point along the coupling cascade or from direct effects on the underlying vasculature.[76] This poses a significant challenge for the use of functional neuroimaging for surgical guidance, as it compromises the validity of the BOLD signal as a biomarker of neural activity. Local zones of NVU-impaired BOLD signal can be interspersed within an otherwise normal pattern of activation. If fMRI is then used by the neurosurgeon to identify eloquent brain tissue near a planned resection site, failure to consider NVU could result in inadvertent resection of healthy tissue. Accordingly, NVU testing is highly recommended when using fMRI for surgical guidance. This may be of particular importance for patients having existing cerebrovascular pathology such as local ischemia, AVMs, highly vascularized tumors, or cerebral infarcts.

Fortunately, testing for NVU is now becoming a more common component of the patient workup for presurgical planning,[76] though the most appropriate method to assess NVU is still under consideration. A method to detect NVU affecting visual cortex is illustrated in Figure 9A–D. The fMRI images in A and B are from a patient with an AVM (white arrow) of the right occipital lobe. The presurgical fMRI maps of visual activation (A and B) show robust left hemisphere activation but little right hemisphere activity (insets indicate color codes for preferred stimulus eccentricity [A] and angular position [B]). Behavioral visual field testing (C) revealed an upper left quadrant vision loss (dark stipple) but normal vision in the lower left quadrant and right hemifield (white stipple). The perimetry pattern of vision loss for this patient was directly compared with the pattern of fMRI activation by computing an FFMap and superimposing it on the perimetry chart (Fig. 9D). Each orange circle in the FFMap corresponds to a voxel in the visual cortex that responded best to a stimulus presented at the circle's location in the visual field (as described earlier). Normally, the FFMap activation and the perimetry should correspond closely. However, for this patient, the preserved vision associated with the lower left quadrant was not matched with a corresponding fMRI response, thereby indicating the presence of NVU (green shading). Had NVU not been detected, the missing fMRI in the right hemisphere might have erroneously suggested that a total resection of the AVM could be performed safely.

An alternate method to detect potential NVU is to use a simple breath-hold (BH) task to map cerebrovascular reactivity (CVR). The BH task induces a transient state of hypercapnia, which normally produces a transient T2* BOLD effect throughout the brain.[76–79] Failure to observe the CVR response in a local region of the brain indicates potential NVU. Figure 9E shows an example of a BH-CVR map in a patient with an expansile nonenhancing WHO grade II glioma (white in the figure) involving the right precentral gyrus. Figure 9F shows fMRI from a tongue movement task used to try to identify eloquent cortex near the tumor. However, the robust fMRI response evident in the left precentral gyrus (large yellow patch with green arrow) is not present in the tumor-infiltrated right hemisphere (left green arrow). (Blue arrows mark central sulcus bilaterally.) One might assume that the lack of fMRI response in or near the tumor indicates that it is safe to resect. However, the BH-CVR map (9E) shows a zone of missing CVR immediately anterior to the tumor (red arrow) despite preserved vascular reactivity (orange) throughout the remaining gray matter. The absent CVR suggests that the lack of a task-induced fMRI response in the right hemisphere was owing to NVU rather than compromised neural function. Indeed, clinical examination revealed that the patient did not have tongue weakness or deviation, consistent with preserved neural function in both the hemispheres.

Conclusion

Task-based fMRI has proven to be a valuable technology for mapping the functional organization of visual cortex in patients having operable brain diseases. Clinically, fMRI can provide key information for planning and guiding brain surgery in patients with pathologies affecting the visual cortex of the occipital, temporal, and parietal lobes. Vision mapping paradigms can provide detailed maps of the retinotopic organization of the visual cortex, thereby permitting identification of brain sites supporting critical central vision in individual patients. FFMaps provide a novel new method to display fMRI brain activation and assess its relationship with existing visual field deficits or to a proposed surgical resection plan through computational “virtual surgery.” FFMaps also can be used to identify regions of NVU, making them additionally valuable for presurgical planning. Physicians should remain cognizant that fMRI is an indirect indicator of neuronal activity, and NVU should always be taken into consideration, especially when it is being used as a biomarker of intact brain tissue. Despite its limitations, fMRI in conjunction with diffusion tensor imaging and other methodologies now provide physicians with an unprecedented array of information that can be used to inform and refine both the diagnosis and treatment of operable pathologies involving the human visual system.

Acknowledgments

This work has been supported in part by NIH, United States, Grants R42NS081926 (DeYoe, Prabhakaran, Prism Clinical Imaging Inc.), R42CA173976 (DeYoe, Pillai, Prism Clinical Imaging Inc.), R01EY024969 (DeYoe), and P30 EY01931. Grateful appreciation to Jed Mathis for help in preparing this manuscript.

References

1. DeYoe, EA., et al. Progress in Cognitive Science: From Cellular Mechanisms to Computational Theories. ZL, Lu, editor. Peking University Press; 2013. p. 414-434.

2. DeYoe EA, Raut RV. Visual mapping using blood oxygen level dependent functional magnetic resonance imaging. Neuroimaging Clin N Am. 2014; 24:573–584. http://dx.doi.Org/10.1016/j.nic.2014.08.001. [PubMed: 25441501]
3. Ulmer JL, Klein AP, Mueller WM, et al. Preoperative diffusion tensor imaging: Improving neurosurgical outcomes in brain tumor patients. Neuroimaging Clin N Am. 2014; 24:599–617. http://dx.doi.Org/10.1016/j.nic.2014.08.002. [PubMed: 25441503]
4. DeYoe, EA., et al. Functional neuroradiology: Principles and clinical applications. Faro, S.; Mohamed, FB., editors. Springer; 2011. p. 485-511.
5. Ulmer, JL., et al. Functional Neuroradiology: Principles and Clinical Applications. Faro, S.; Mohamed, FB., editors. Springer; 2011. p. 731-765.
6. Biswal BB, et al. Towards discovery science of human brain function: The '1000 Connectomes' Project. 2010
7. Van Essen DC, et al. The WU-Minn Human Connectome Project: An overview. Neuroimage. 2013; 80:62–79. http://dx.doi.org/10.1016/j.neuroimage.2013.05.041. [PubMed: 23684880]
8. Zeki S. Cerebral akinetopsia (visual motion blindness). Brain. 114:811–824. [PubMed: 2043951]
9. Zeki S. A century of cerebral achromatopsia. Brain. 1990; 113:1721–1777. [PubMed: 2276043]
10. Benevento LA, Rezak M. The cortical projections of the inferior pulvinar and adjacent lateral pulvinar in the rhesus monkey (*Macaca mulatto*): An autoradiographic study. Brain Res. 1976; 108:1–24. [PubMed: 819095]
11. Hendrickson, A.; Edwards, SB. Neuroanatomical Research Techniques. R. T. Robertson, Academic Press; 1978. The use of axonal transport for autoradiographic tracing of pathways in the central nervous system; p. 241-289.
12. Lund JS, Lund RD, Hendrickson AE, et al. The origin of efferent pathways from the primary visual cortex, area 17, of the macaque monkey as shown by retrograde transport of horseradish peroxidase. J Comp Neurol. 1975; 164:287–304. [PubMed: 810501]
13. Mesulam, M-M. Tracing Neural Connections with Horseradish Peroxidase. New York: Wiley; 1982. p. 63-69.
14. Ungerleider, LG.; Mishkin, M.; Goodale, MA., et al. Analysis of Visual Behavior. Ingle, DJ., editor. MIT Press; 1982. p. 549-586.
15. Milner AD, Goodale MA. Two visual systems re-viewed. Neuropsychologia. 2008; 46:774–785. [PubMed: 18037456]
16. Horton JC, Hoyt WF. The representation of the visual field in human striate cortex. A revision of the classic Holmes map. Arch Ophthalmol. 1991; 109:816–824. [PubMed: 2043069]
17. Horton JC, Hoyt WF. Quadrantic visual field defects: A hallmark of lesions in extrastriate (V2/V3) cortex. Brain. 1991; 114:1703–1718. [PubMed: 1884174]
18. Tootell RBH, et al. Functional analysis of V3A and related areas in human visual cortex. J Neurosci. 1997; 17:7060–7078. [PubMed: 9278542]
19. Smith AT, Greenlee MW, Singh KD, et al. The processing of first- and second-order motion in human visual cortex assessed by functional magnetic resonance imaging (fMRI). J Neurosci. 1998; 18:3816–3830. [PubMed: 9570811]
20. Greenlee MW, Smith AT. Detection and discrimination of first- and second-order motion in patients with unilateral brain damage. J Neurosci. 1997; 17:804–818. [PubMed: 8987802]
21. Brouwer GJ, van Ee R. Visual cortex allows prediction of perceptual states during ambiguous structure-from-motion. J Neurosci. 2007; 27:1015–1023. [PubMed: 17267555]
22. Tsao DY, et al. Stereopsis activates V3A and caudal intraparietal areas in macaques and humans. Neuron. 2003; 39:555–568. [PubMed: 12895427]
23. Watson JDG, et al. Area V5 of the human brain: Evidence from a combined study using positron emission tomography and magnetic resonance imaging. Cereb Cortex. 1993; 3:79–94. [PubMed: 8490322]
24. Tootell RB, et al. Functional analysis of human MT and related visual cortical areas using magnetic resonance imaging. J Neurosci. 1995; 15:3215–3230. [PubMed: 7722658]
25. Zihl J, Von Cramon D, Mai N, et al. Disturbance of movement vision after bilateral posterior brain damage. Brain. 1991; 114:2235–2252. [PubMed: 1933243]

26. Rosa MG, Tweedale R. The dorsomedial visual areas in New World and Old World monkeys: Homology and function. Eur J Neurosci. 2001; 13:421–427. [PubMed: 11168549]
27. Pitzalis S, et al. Human V6: The medial motion area. Cereb Cortex. 2009
28. Howard RJ, et al. A direct demonstration of functional specialization within motion-related visual and auditory cortex of the human brain. Curr Biol. 1996; 6:1015–1019. [PubMed: 8805334]
29. Grossman ED, Blake R. Brain activity evoked by inverted and imagined biological motion. Vision Res. 2001; 41:1475–1482. [PubMed: 11322987]
30. Downing PE, Jiang Y, Shuman M, et al. A cortical area selective for visual processing of the human body. Science. 2001; 293:2470–2473. [PubMed: 11577239]
31. Peelen MV, Wiggett AJ, Downing PE. Patterns of fMRI activity dissociate overlapping functional brain areas that respond to biological motion. Neuron. 2006; 49:815–822. [PubMed: 16543130]
32. Tootell RBH, et al. The retinotopy of spatial attention. Neuron. 1998; 21:1409–1422. [PubMed: 9883733]
33. Corbetta M, Kincade MJ, Lewis C, et al. Neural basis and recovery of spatial attention deficits in spatial neglect. Nat Neurosci. 2005; 8:1603–1610. [PubMed: 16234807]
34. Corbetta M, Patel G, Shulman GL. The reorienting system of the human brain: From environment to theory of mind. Neuron. 2008; 58:306–324. [PubMed: 18466742]
35. Mesulam MM. Spatial attention and neglect: Parietal, frontal and cingulate contributions to the mental representation and attentional targeting of salient extrapersonal events. Philos Trans R Soc Lond B Biol Sci. 1999; 354:1325–1346. [PubMed: 10466154]
36. Merigan W, Freeman A, Meyers SP. Parallel processing streams in human visual cortex. Neuroreport. 1997; 8:3985–3991. [PubMed: 9462479]
37. Merigan WH, Pham HA. V4 lesions in macaques affect both single- and multiple-viewpoint shape discriminations. Vis Neurosci. 1998; 15:359–367. [PubMed: 9605535]
38. Merigan WH. Cortical area V4 is critical for certain texture discriminations, but this effect is not dependent on attention. Vis Neurosci. 2000; 17:949–958. [PubMed: 11193111]
39. Grill-Spector K, et al. A sequence of object-processing stages revealed by fMRI in the human occipital lobe. Hum Brain Mapp. 1998; 6:316–328. [PubMed: 9704268]
40. Kastner S, De Weerd P, Ungerleider LG. Texture segregation in the human visual cortex: A functional MRI study. J Neurophysiol. 2000; 83:2453–2457. [PubMed: 10758146]
41. Wade A, Augath M, Logothetis N, et al. fMRI measurements of color in macaque and human. J Vis. 2008; 8(6):1–19.
42. McKeefry DJ, Zeki S. The position and topography of the human colour centre as revealed by functional magnetic resonance imaging. Brain. 1997; 120:2229–2242. [PubMed: 9448578]
43. Beauchamp MS, Haxby JV, Jennings JE, et al. An fMRI version of the Farnsworth-Munsell 100-Hue test reveals multiple color-selective areas in human ventral occipitotemporal cortex. Cereb Cortex. 1999; 9:257–263. [PubMed: 10355906]
44. Brewer AA, Liu J, Wade AR, et al. Visual field maps and stimulus selectivity in human ventral occipital cortex. Nat Neurosci. 2005; 8:1102–1109. [PubMed: 16025108]
45. Liu J, Wandell BA. Specializations for chromatic and temporal signals in human visual cortex. J Neurosci. 2005; 25:3459–3468. [PubMed: 15800201]
46. Kanwisher N, McDermott J, Chun MM. The fusiform face area: A module in human extrastriate cortex specialized for face perception. J Neurosci. 1997; 17:4302–4311. [PubMed: 9151747]
47. Steeves JK, et al. The fusiform face area is not sufficient for face recognition: Evidence from a patient with dense prosopagnosia and no occipital face area. Neuropsychologia. 2006; 44:594–609. [PubMed: 16125741]
48. Epstein R, Harris A, Stanley D, et al. The parahippocampal place area: Recognition, navigation, or encoding? Neuron. 1999; 23:115–125. [PubMed: 10402198]
49. Epstein R, DeYoe EA, Press DZ, et al. Neuropsychological evidence for a topographical learning mechanism in parahippocampal cortex. Cogn Neuropsychol. 2001; 18:481–508. [PubMed: 20945226]
50. Cohen L, Dehaene S. Specialization within the ventral stream: The case for the visual word form area. Neuroimage. 2004; 22:466–476. [PubMed: 15110040]

51. Paus T. Location and function of the human frontal eye-field: A selective review. Neuropsychologia. 1996; 34:475–483. [PubMed: 8736560]
52. Hagler DJ Jr, Sereno MI. Spatial maps in frontal and prefrontal cortex. Neuroimage. 2006; 29:567–577. [PubMed: 16289928]
53. Gill, S.; Ulmer, J.; DeYoe, EA. Vision and Higher Cortical Function. In: Holodny, AI., editor. Functional Neuroimaging: A Clinical Approach. Informa Healthcare; 2008. p. 67-80.
54. DeYoe EA, Raut RV. Visual mapping using BOLD fMRI. Neuroimaging Clin N Am. 2014; 24:573–584. [PubMed: 25441501]
55. Hirsch J, et al. An integrated functional magnetic resonance imaging procedure for preoperative mapping of cortical areas associated with tactile, motor, language, and visual functions. Neurosurgery. 2000; 47:711–721. [discussion 721-712]. [PubMed: 10981759]
56. Kapsalakis IZ, et al. Preoperative evaluation with FMRI of patients with intracranial gliomas. Radiol Res Pract. 2012; 2012:727810. http://dx.doi.org/10.1155/2012/727810. [PubMed: 22848821]
57. Cohen L, et al. The visual word form area: Spatial and temporal characterization of an initial stage of reading in normal subjects and posterior split-brain patients. Brain. 2000; 123(Pt 2):291–307. [PubMed: 10648437]
58. Price CJ, Devlin JT. The myth of the visual word form area. Neuroimage. 2003; 19:473–481. [PubMed: 12880781]
59. Krauzlis RJ. The control of voluntary eye movements: New perspectives. Neuroscientist. 2005; 11:124–137. http://dx.doi.org/10.1177/1073858404271196. [PubMed: 15746381]
60. Henderson JM. Human gaze control during real-world scene perception. Trends Cogn Sci. 2003; 7:498–504. [PubMed: 14585447]
61. Das A, Huxlin KR. New approaches to visual rehabilitation for cortical blindness: Outcomes and putative mechanisms. Neuroscientist. 2010; 16:374–387. http://dx.doi.org/10.1177/1073858409356112. [PubMed: 20103505]
62. Das A, Demagistris M, Huxlin KR. Different properties of visual relearning after damage to early versus higher-level visual cortical areas. J Neurosci. 2012; 32:5414–5425. http://dx.doi.org/10.1523/JNEUROSCI.0316-12.2012. [PubMed: 22514305]
63. Reitsma DC, et al. Atypical retinotopic organization of visual cortex in patients with central brain damage: Congenital and adult onset. J Neurosci. 2013; 33:13010–13024. http://dx.doi.org/10.1523/JNEUROSCI.0240-13.2013. [PubMed: 23926256]
64. Guillery RW. Visual pathways in albinos. Sci Am. 1974; 230:44–54. [PubMed: 4822986]
65. Guillery RW, Okoro AN, Witkop CJ Jr. Abnormal visual pathways in the brain of a human albino. Brain Res. 1975; 96:373–377. [PubMed: 1175020]
66. Summers CG. Vision in albinism. Trans Am Ophthalmol Soc. 1996; 94:1095–1155. [PubMed: 8981720]
67. Morland AB, Hoffmann MB, Neveu M, et al. Abnormal visual projection in a human albino studied with functional magnetic resonance imaging and visual evoked potentials. J Neurol Neurosurg Psychiatry. 2002; 72:523–526. [PubMed: 11909915]
68. Hoffmann MB, Tolhurst DJ, Moore AT, et al. Organization of the visual cortex in human albinism. J Neurosci. 2003; 23:8921–8930. [PubMed: 14523094]
69. Victor JD, et al. Visual function and brain organization in non-decussating retinal-fugal fibre syndrome. Cereb Cortex. 2000; 10:2–22. [PubMed: 10639391]
70. Hoffmann MB, et al. Plasticity and stability of the visual system in human achiasma. Neuron. 2012; 75:393–401. http://dx.doi.Org/10.1016/j.neuron.2012.05.026. [PubMed: 22884323]
71. Sinha P, Meng M. Superimposed hemifields in primary visual cortex of achiasmic individuals. Neuron. 2012; 75:353–355. http://dx.doi.org/10.1016/j.neuron.2012.07.003. [PubMed: 22884317]
72. Huang K, Guillery RW. A demonstration of two distinct geniculocortical projection patterns in albino ferrets. Brain Res. 1985; 352:213–220. [PubMed: 4027667]
73. Logothetis NK. The underpinnings of the BOLD functional magnetic resonance imaging signal. J Neurosci. 2003; 23:3963–3971. [PubMed: 12764080]

74. Attwell D, et al. Glial and neuronal control of brain blood flow. Nature. 2010; 468:232–243. [PubMed: 21068832]
75. Hillman EM. Coupling mechanism and significance of the BOLD Signal: A status report. Annu Rev Neurosci. 2014; 37:161–181. http://dx.doi.org/10.1146/annurev-neuro-071013-014111. [PubMed: 25032494]
76. Pillai, JJ.; Mikulis, DJ. Cerebrovascular reactivity mapping: An evolving standard for clinical functional imaging. Am J Neuroradiol. http://dx.doi.org/10.3174/ajnr.A3941
77. Pillai JJ, Zaca D. Clinical utility of cerebrovascular reactivity mapping in patients with low grade gliomas. World J Clin Oncol. 2011; 2:397–403. [PubMed: 22171282]
78. Zaca D, Hua J, Pillai JJ. Cerebrovascular reactivity mapping for brain tumor presurgical planning. World J Clin Oncol. 2011; 2:289–298. [PubMed: 21773079]
79. Pillai JJ, Zaca D. Comparison of BOLD cerebrovascular reactivity mapping and DSC MR perfusion imaging for prediction of neurovascular uncoupling potential in brain tumors. Technol Cancer Res Treat. 2012
80. Wandell BA, Winawer J. Imaging retinotopic maps in the human brain. Vis Res. 2010
81. Malach R, et al. Object-related activity revealed by functional magnetic resonance imaging in human occipital cortex. Proc Natl Acad Sci U S A. 1995; 92:8135–8139. [PubMed: 7667258]
82. Swisher JD, Halko MA, Merabet LB, et al. Visual topography of human intraparietal sulcus. J Neurosci. 2007; 27:5326–5337. [PubMed: 17507555]
83. Konen CS, Kastner S. Representation of eye movements and stimulus motion in topographically organized areas of human posterior parietal cortex. J Neurosci. 2008; 28:8361–8375. [PubMed: 18701699]
84. Felleman DJ, Van Essen DC. Distributed hierarchical processing in the primate cerebral cortex. Cereb Cortex. 1991; 1:1–47. [PubMed: 1822724]
85. Balasubramanian M, Polimeni J, Schwartz EL. The V1-V2-V3 complex: Quasiconformal dipole maps in primate striate and extra-striate cortex. Neural Netw. 2002; 15:1157–1163. [PubMed: 12425434]

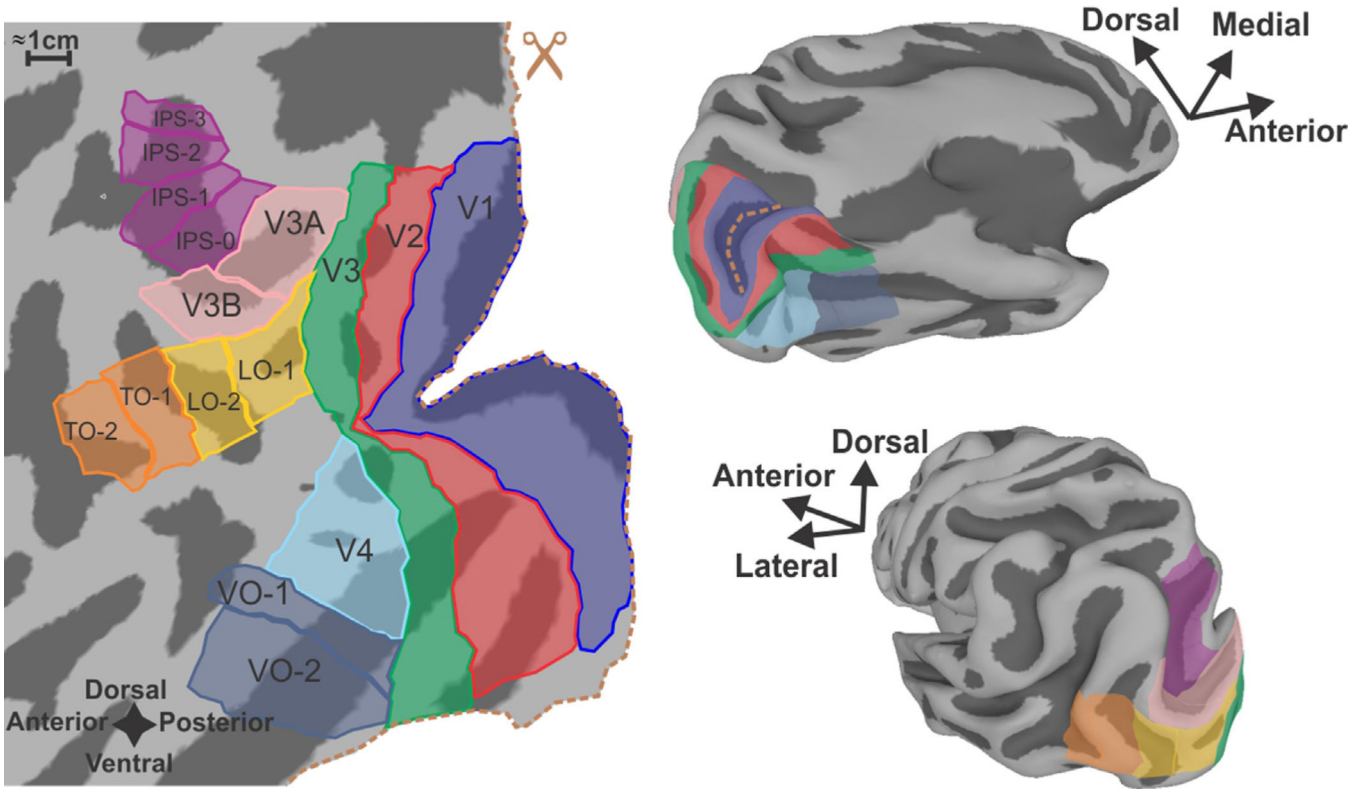

Figure 1.

Subdivisions of the human visual cortex displayed on cortical surface models of an individual subject. At left is a cortical flat map created by computationally unfolding the occipital lobe portion of the 3D surface model shown on the right. (Dotted orange line along the right margin of the flat map marks edges of a computational "cut" along the fundus of the calcarine sulcus, which is shaded navy blue on the upper 3D model. The cut allows the surface to unfold with less distortion.) Dark gray zones on all models represent the interior of sulci. Colored patches mark approximate locations of functionally distinct visual areas. Primary visual cortex (a.k.a. VI, striate cortex)—navy blue. V2—red. V3—green. V4—light blue. Ventral occipital complex[80]—blue-gray. Lateral occipital complex[39,81]—yellow. Temporal Occipital complex (a.k.a. hMT+, MST)[80]—orange. V3A/B[18–22]—pink. IPSO (a.k.a. V7); IPS1-3[82–83]—magenta. It should be noted that the region in and around the VO complex may be composed of multiple visual areas such as the visual word-form area[50] and the fusiform face area[46] defined differently by other investigators. (Color version of figure is available online.)

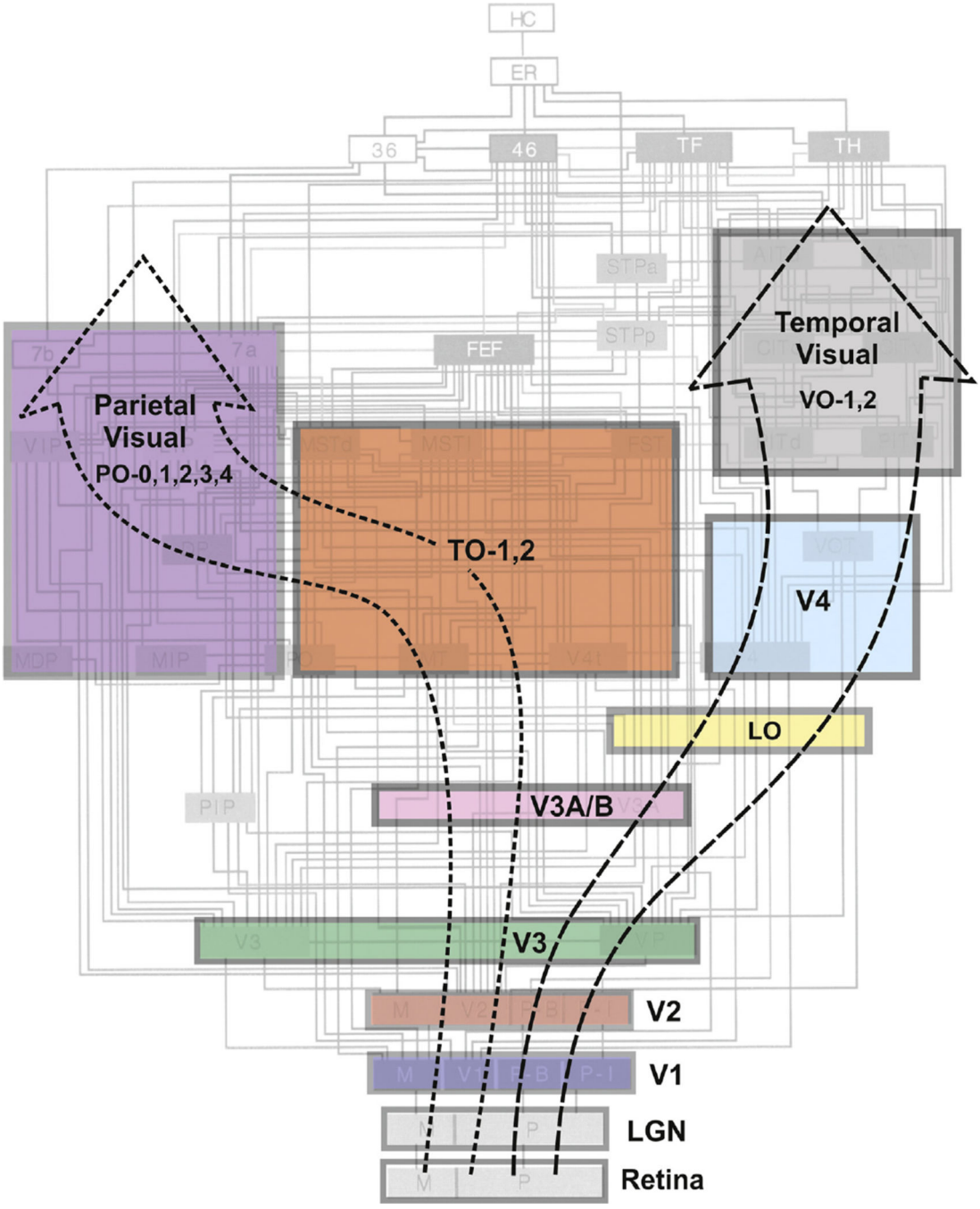

Figure 2.

A simplified diagram of presumed visual processing streams in the human cerebral cortex. Colored boxes indicate individual visual areas or groups of visual areas that have been identified in humans and correspond to those shown in Figure 1. (Sizes of boxes do not indicate relative physical size or functional importance.) Large dashed arrows indicate groups of areas that, by analogy with nonhuman primates, are likely to be interconnected to form 2 major visual processing streams feeding into parietal cortex (dorsal “what-how” stream) and temporal cortex (ventral “what” stream). Visual area boxes are overlaid on

roughly corresponding portions of a connectional diagram of a macaque monkey's visual areas based on Felleman and Van Essen[84] that provides an estimate of the 2 dozen + visual areas and interconnecting pathways that eventually may be identified in humans, though departures from the macaque pattern are anticipated. Hierarchical positions of some human areas (eg, V3A/B and LO) may differ from those shown. Each major stream has multiple functional substreams and the 2 streams have many cross-connections. Additional or alternate human areas have been proposed, and the nomenclature of some areas can vary (see Fig. 1 and Table for nomenclature used here). LGN, lateral geniculate nucleus. (Color version of figure is available online.)

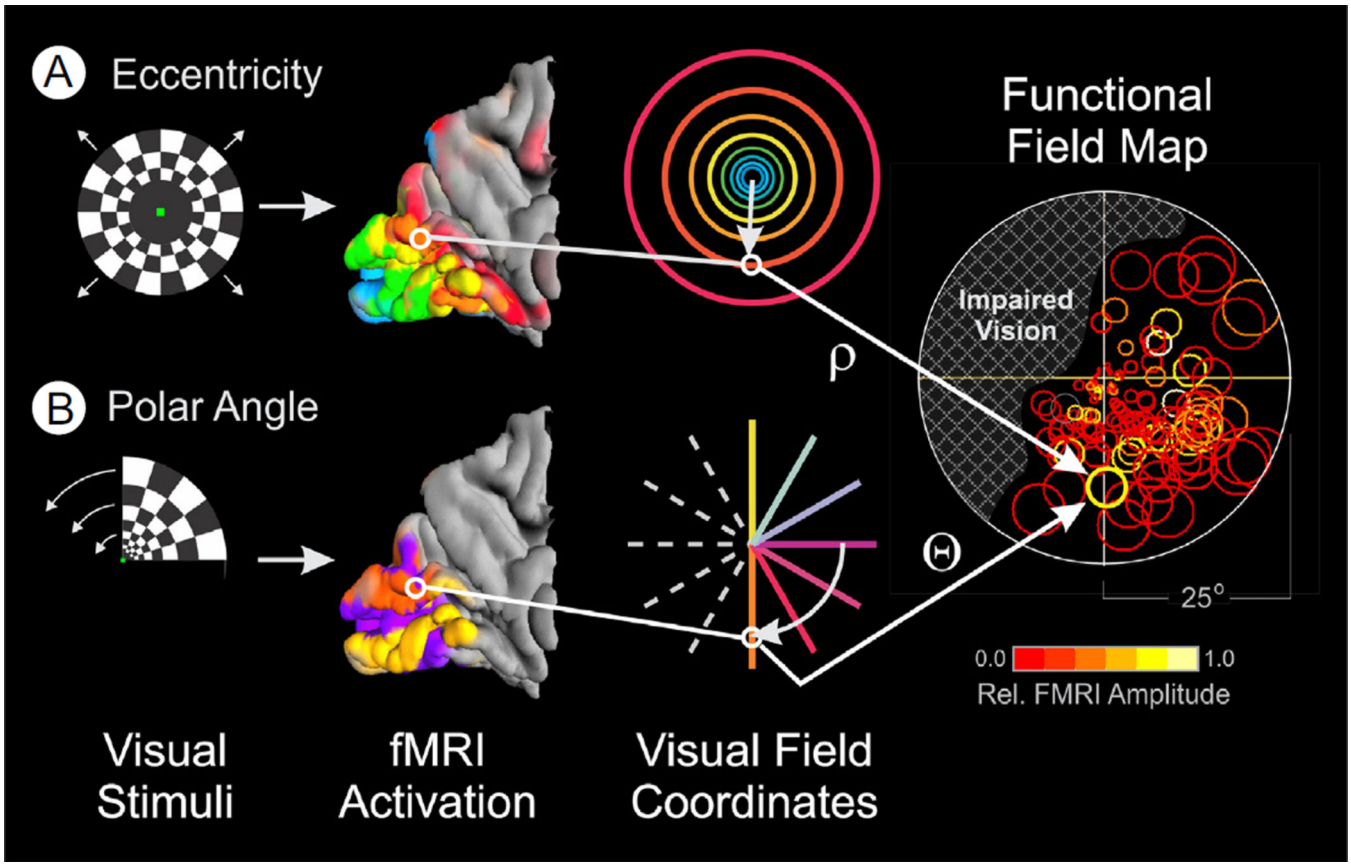

Figure 3.

Stimuli for visual field mapping and construction of functional field maps (FFMaps). Retinotopic mapping stimuli consist of an expanding, black-and-white, checkered annulus (A) or a rotating wedge (B) counterphase flickered at 6 Hz and presented in a temporal phase mapping paradigm. A single expansion-rotation sequence takes 32 seconds and is repeated 5 times within a 168-second scan run. (The initial 8 seconds of the scan containing the equilibration transient are discarded.) The outer boundary of the stimuli extends to approximately 25° eccentricity. Expanding annuli are not scaled linearly in size and eccentricity but, rather, are scaled nonlinearly so as to activate roughly equal areas of V1, as estimated using the retinocortical mapping function by Balasubramanian et al.[85] The subject's task during each mapping sequence is to fixate a small dot at the center of the display and press a button when the dot blinks off for 0.125 seconds, varied randomly every 4-8 seconds. This task helps ensure that the patient attends to the mapping stimulus and maintains gaze at the center of the display. Postprocessing of the resulting fMRI data yields an estimate of the visual field coordinates (eccentricity [rho], angle [theta]) at which the mapping stimuli activate each voxel most strongly. Using these coordinates, a circle symbol can be placed at the corresponding location on a diagram of the patient's view of the stimulus display (right). The symbol is colored to show the amplitude of the fMRI response according to the pseudocolor scale below the FFMap. The size of the symbol represents the error in estimating the preferred stimulus location for that voxel (approximately 70% confidence interval). Symbols for all visually responsive voxels are placed on the diagram to

yield an FFMap that allows the physician to determine instantly if the patient's visual cortex is responding to all locations within his or her field of view or if there is a zone of impaired brain response, indicated here by cross-hatching in the upper left field. (Color version of figure is available online.)

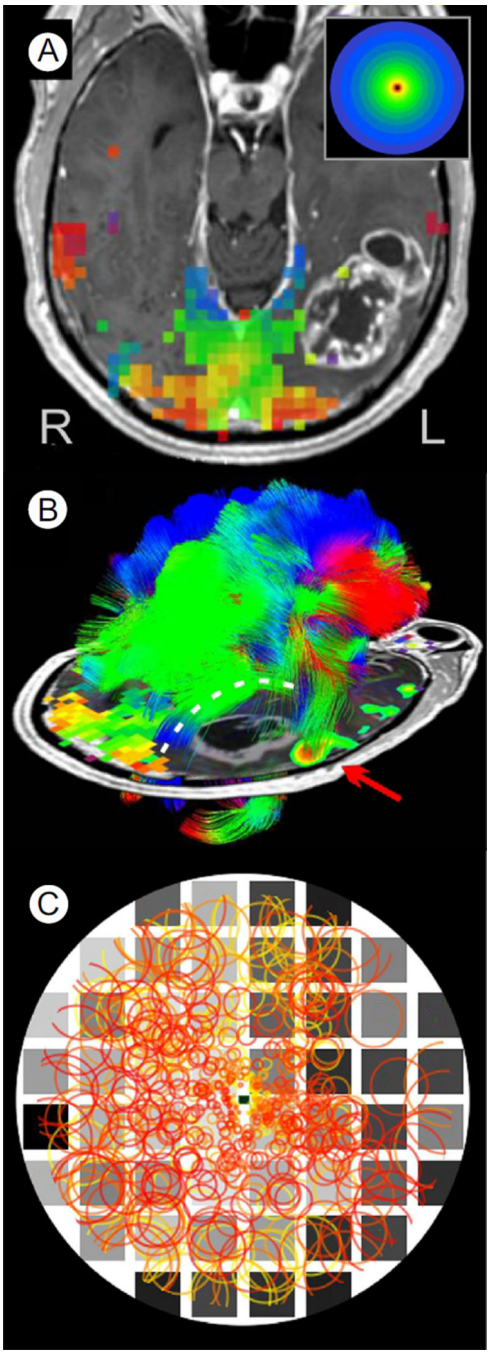

Figure 4.

fMRI vision mapping, diffusion tensor tractography, and FFMap for a patient with an occipitotemporal tumor. (A) Postcontrast T1-weighted, axial section through the occipital visual cortex showing fMRI activation in response to the expanding ring stimulus. Visually, active voxels (squares) are color coded (inset shows key) to indicate the eccentricity of the stimulus ring that maximally activated each voxel. Voxels representing the center of gaze are colored red or orange, with voxels representing increasingly eccentric portions of the field colored yellow, green, and blue. A tumor mass is evident in the left occipitotemporal

region. (B) Diffusion tensor imaging tractography color coded by maximum diffusion direction for each voxel. Optic radiations (white dashed line), which have been displaced dorsally, arch over the tumor region to innervate visually responsive posterior cortex. An embedded 2D axial image shows the location of tumor visible in this single section below the arching optic radiations. Also shown is a lateral fMRI focus (red arrow) activated by a language task. Proximity of the language focus, the optic radiations, and the presumed visual word-form area (not shown) were key landmarks used to guide the subsequent surgical resection of the tumor. (C) Functional Field Map showing the fMRI pattern of visual response (circle symbols) computationally projected onto a diagram of the patient's visual field. Underlay is a visual perimetry chart showing locations of normal visual sensitivity (light gray squares) and impaired sensitivity (dark gray, black squares). It should be noted that visual sensitivity, as measured behaviorally, was impaired throughout much of the right visual field, especially in the upper quadrant. fMRI activation represented by the circle symbols was also sparse in the lateral portion of the right hemifield. However, normal levels of activation (circle symbol density) were observed closer to the vertical meridian, suggesting that the reduced visual sensitivity in the right upper quadrant was not solely due to impairment of the incoming retinal signals. This was consistent with the preserved yet displaced optic radiations evident in the tractography (B). (Color version of figure is available online.)

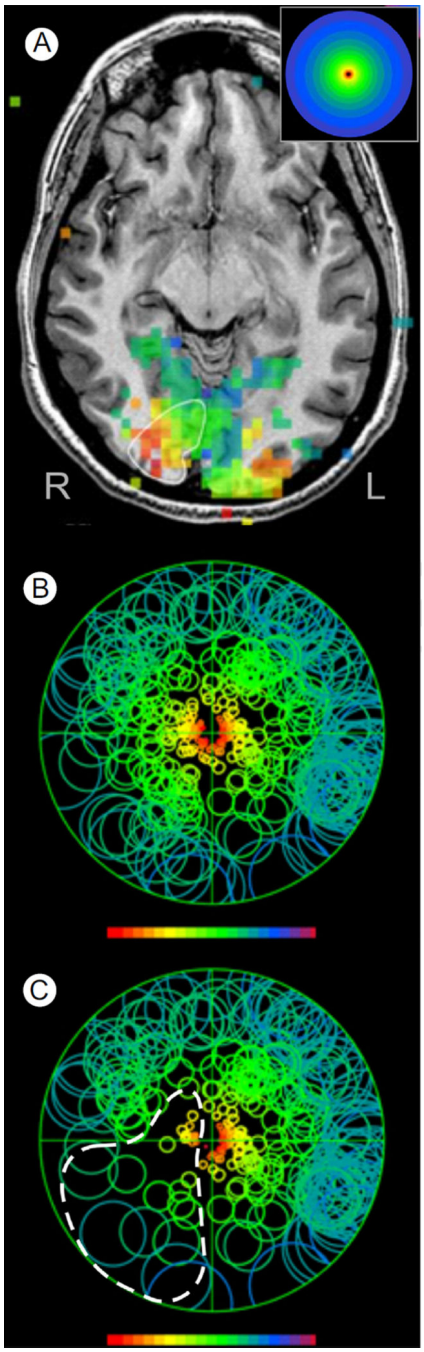

Figure 5.

"Virtual surgery" used to estimate potential treatment-induced vision loss. (A) T1-weighted anatomical image with superimposed fMRI vision mapping. Visually active voxels (squares) are color coded (inset shows key) to indicate the eccentricity of the stimulus ring that maximally activated each voxel. The thin white outline shows the planned resection zone containing an obviously eloquent portion of the visual cortex. (B) FFMap constructed from the fMRI activation of A plus a complementary mapping of visual field angular preference (not shown) based on the rotating wedge stimulus. Circle symbols are pseudocolored using

the same color code shown by the inset to figure A to emphasize the correspondence of the FFMap symbols with the fMRI activation in the brain. (C) The same FFMap but after all active voxels within the planned resection zone have been removed by computational "virtual surgery." The dashed white outline surrounds the portion of the patient's visual field that might be impaired (reduced symbol density) by the planned resection. Though many factors (eg, collateral tissue damage at a distance from the resection) might compromise the accuracy of this estimate, this case illustrates the potential to provide surgical guidance at a level of sophistication that was not previously possible. (Color version of figure is available online.)

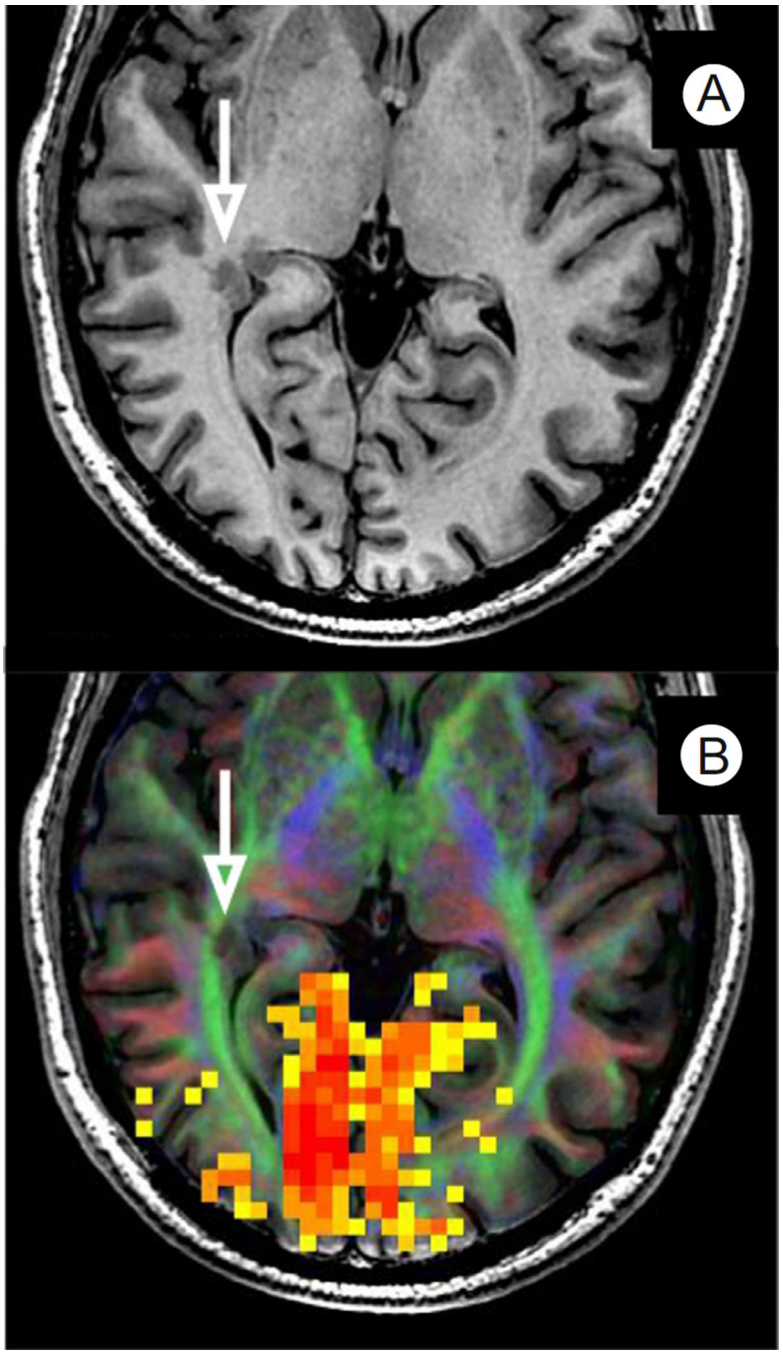

Figure 6.

fMRI visual mapping in a patient with gray matter heterotopia. (A) A T1-weighted axial anatomical image showing gray matter heterotopia (white arrow) in an epileptic patient with poorly controlled seizures. (B) A DTI tractography orientation map (colored white matter) shows that the heterotopia extends into the adjacent optic radiations (green) that provide the retinal sensory input, driving the visually driven fMRI activation (red or yellow voxels) in the same hemisphere. The heterotopia was not targeted for resection. See text for outcome and additional case details. (Color version of figure is available online.)

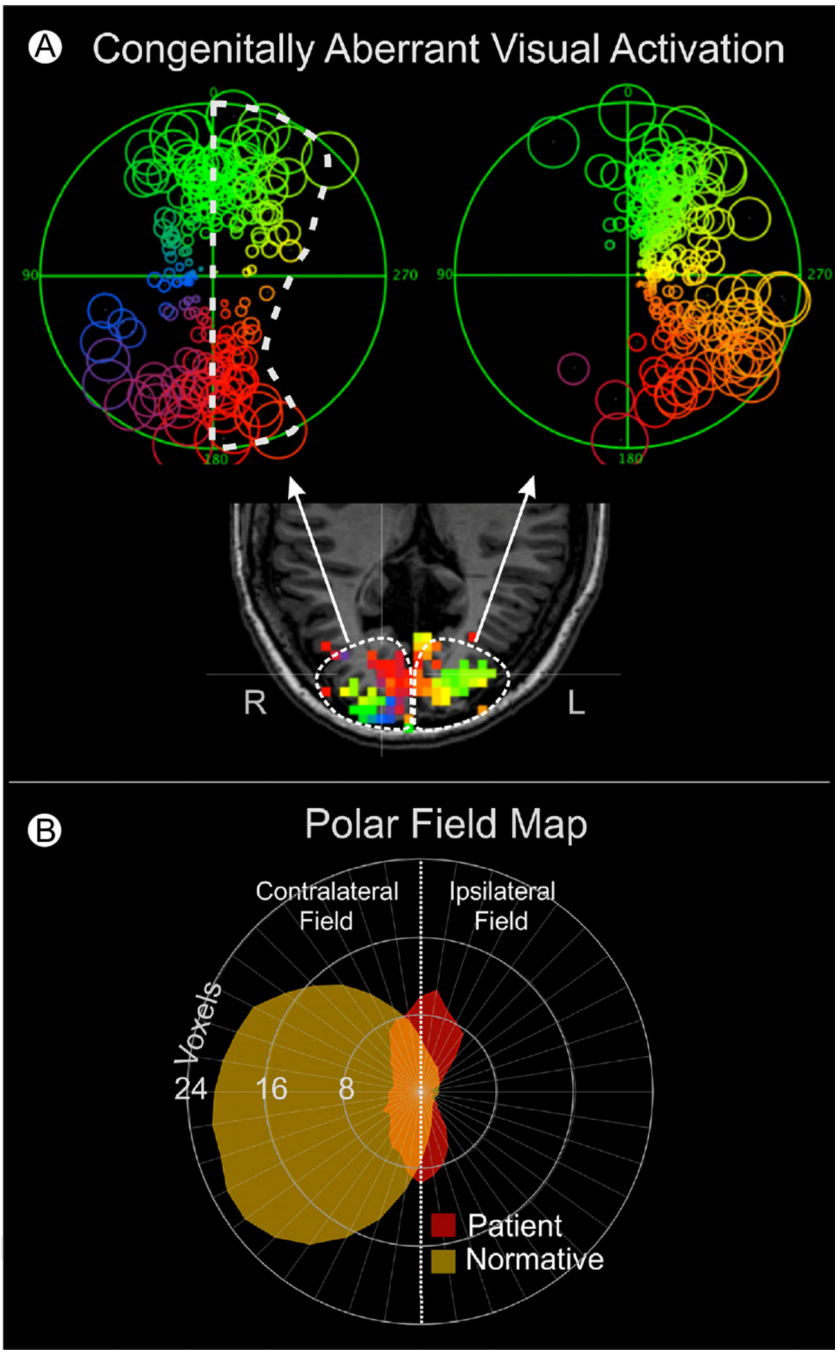

Figure 7.

Congenitally aberrant visual cortex activation in a patient with childhood hydrocephalus. (A) Functional Field Maps computed from fMRI activation of each hemisphere separately. The FFMap at the right of the figure was computed from the left hemisphere and consists of a normal hemifield representation (but with some loss in the upper right quadrant). In contrast, the FFMap at the left of the figure was computed from the right hemisphere and shows a very reduced representation of the normal contralateral (left) visual field but a highly expanded, yet aberrant, representation of the ipsilateral (right) visual field

(surrounded by white dashed outline). (B) Quantitative comparison of this patient's right hemisphere representation of the visual field (red) with the average right hemisphere representation for a group of healthy control subjects (yellow). Each data point on the circumference of such a polar field map represents the number of visually active voxels contained within a thin radial “pie wedge” of visual field extending radially at the same angle as the data point. For example, approximately 22 voxels (between 16 and 24) were found to represent the left horizontal meridian of healthy subjects, whereas the patient data yielded approximately 4 voxels. It should be noted that for normal, healthy subjects, very few voxels in the right hemisphere represent the ipsilateral field (to the right of the vertical meridian). However, for this patient, nearly half of the voxels in the right hemisphere represent the ipsilateral field. (Adapted with permission from Reitsma et al.[63]) (Color version of figure is available online.)

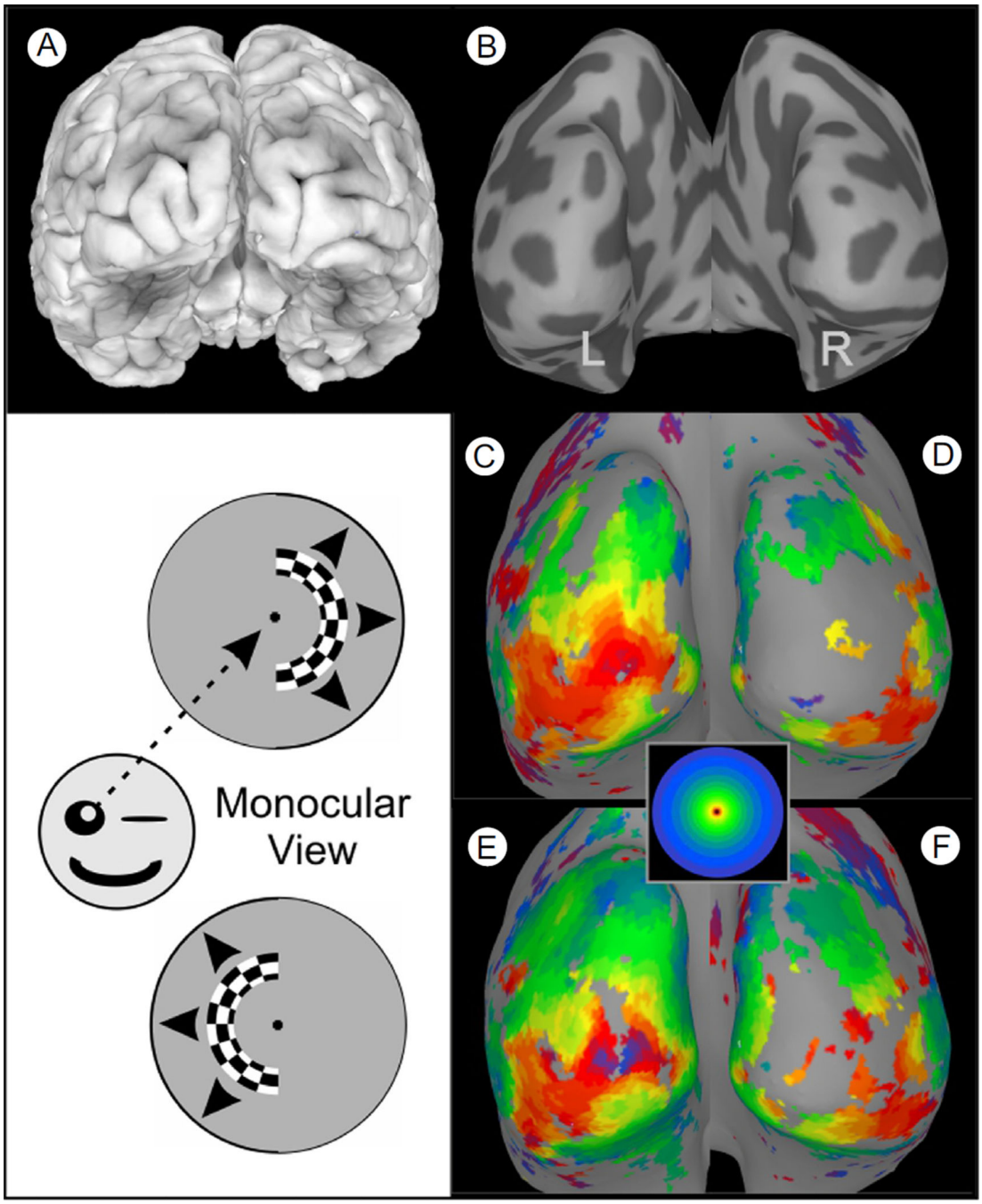

Figure 8.

Aberrant cortical maps in albinism. (A) Posterior view of a 3-dimensional cortical surface model of an albinistic patient's brain. (B) A smoothed cortical surface model obtained by computationally “inflating” the surface model of A. Dark gray patches represent the interior of sulci. (C and D) Left and right hemisphere surface maps showing the pattern of fMRI activation produced when the expanding ring stimulus was confined to the right visual field and viewed monocularly with the right eye (as depicted by the schematic directly to the left). This produced activation that was largely confined to the left hemisphere, contralateral to

the stimulus, as would be the case for a nonalbinistic subject. However, when the checkered hemiring was presented in the left visual field (lower schematic), the resulting pattern of activation was, again, strongest and most complete in the left hemisphere (now ipsilateral to the stimulus). Thus, for an albinistic patient, opposite halves of the visual field projected onto the same, left occipital cortex. Note: The aberrant mapping in albinism is not typically apparent if the stimuli are viewed binocularly, because the opposite eye “fills in” the pattern for the opposite hemisphere. (Color version of figure is available online.)

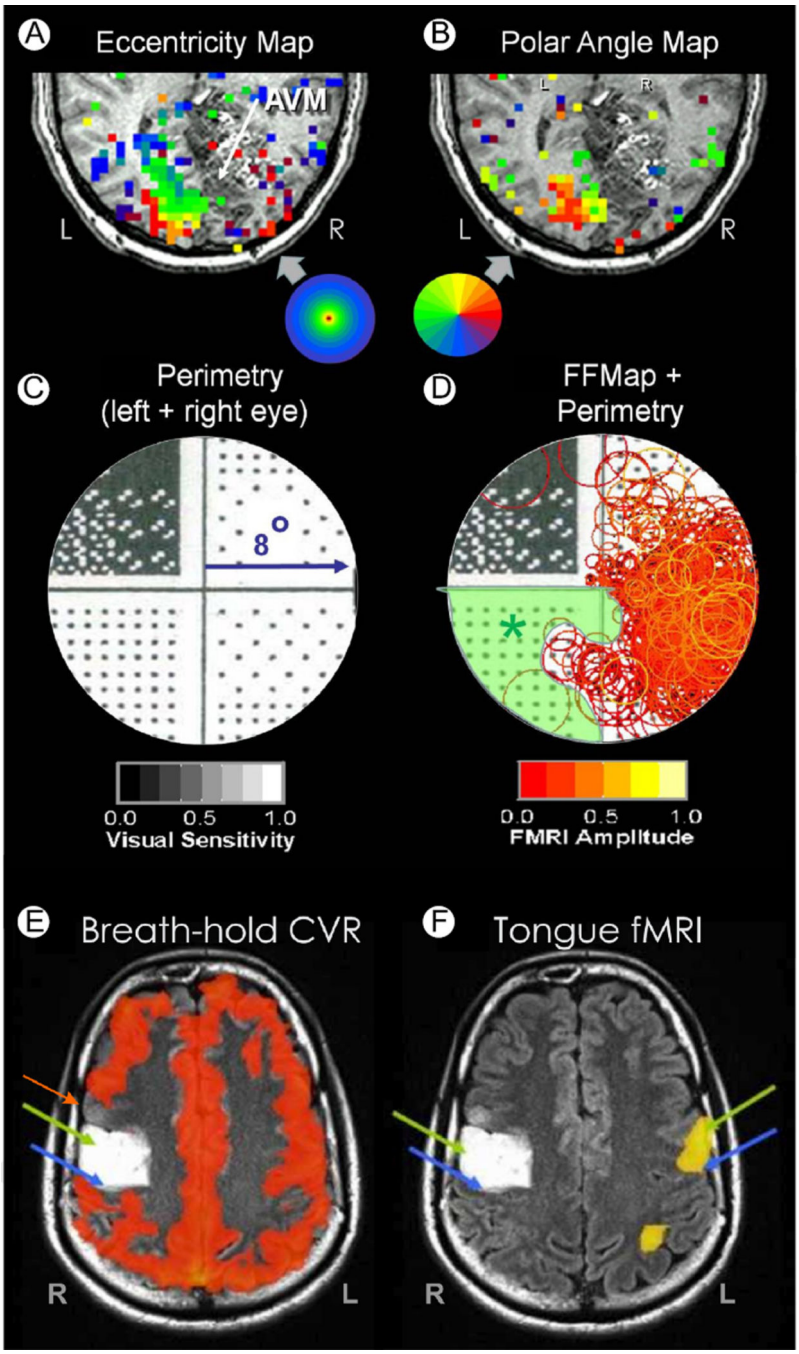

Figure 9.

Neurovascular uncoupling. (A) fMRI-based eccentricity mapping (ring stimuli) in the visual cortex of a patient with an arteriovenous malformation in the right occipitoparietal cortex. fMRI activation is color coded to indicate the eccentricity of the ring stimulus that most strongly activated each voxel (inset shows color code). (B) fMRI mapping of visual field polar angle (inset shows color code). (C) Humphrey perimetry of the central 8° showing an upper left quadrantanopsia. (D) Functional field map showing robust fMRI activation (orange circles) limited mainly to the right visual field. However, the Humphrey perimetry

chart in the background indicates that vision is normal (sparse stipple) in the lower left quadrant, thus marking a zone of missing BOLD activation due to neurovascular uncoupling (green shading). (E) BOLD T2* map of cerebrovascular reactivity (CVR) in response to a breath-hold task for a patient with a glioma in the right precentral gyrus (white zone). (F) fMRI activation induced by a tongue movement task should activate motor cortex bilaterally. However, lack of CVR response within (green arrow) and anterior (red arrow) to the tumor suggests a potential zone of neurovascular uncoupling. Blue arrows mark central sulcus in both E and F. (Color version of figure is available online.)

Table

Some Perceptual Contributions of Human Cortical Visual Areas

Cortical Area	Location	Perceptual Function	Effects of Damage	References
Early stages				
V1	See Figure 1	Low-level rep of most visual features	Scotoma	16
V2	See Figure 1	Low-level rep of most visual features	Scotoma	17
V3	See Figure 1	Low-level rep of many visual features	Scotoma?	17
V3A/B	See Figure 1	Complex motion, SFM (V3A), and stereopsis	?	18–22
Dorsal stream				
TO-1,2 (hMT+/V5)	See Figure 1	Object trajectory, complex motion, and SFM	Akinetopsia	21,23–25
V6	Dorsal POS	Self-motion and motion flow	?	26,27
BMA	Posterior STS	Biological motion	Impaired biomotion percept?	28,29
EBA	Posterior ITS	Static body and limbs	?	30,31
IPSO (V7)	See Figure 1	Saccadic eye movements, SFM, and stereopsis	?	21,22,32
IPS1-3CLIP+)	See Figure 1	Saccadic eye movements and attention control	Neglect	33–35
Ventral stream				
V4	See Figure 1	Form and texture	Impaired texture and form perception	36–41
LO-1,2	See Figure 1	Object form, cue-invariant form, and fig/gnd	Object agnosias	39
VO-1,2	See Figure 1	Color and form (may overlap with FFA and WFA)	Achromatopsia and object agnosias	42–45
FFA	p. Fusiform g.	Face perception and high-level form discrimination	Prosopagnosia	46,47
PPA	Parahippoc. g.	Encode layout of environmental space	Impaired encoding of spatial layout	48,49
WFA	Fusiform g.	Visual recognition of words	Word-form agnosia	50
Frontal				
FEF	SFS/PCSj.	Eye movements and spatial attention	Impaired eye movements and neglect	33–35,51,52
DLPFC+	IFS/PCS	Work memory and spatial attention	Neglect	33–35,52

Nomenclature for particular cortical areas generally follows that used in the references cited in the far right column. The anatomical locations of particular visual areas other than V1 are approximate and can vary from individual to individual. Positive identification of individual visual areas in a particular patient may require converging evidence from fMRI, DTI, and lesion-related symptomatology. Perceptual functions listed for specific visual areas are typically the result of neuronal activity in a connectional subnetwork of hierarchically interconnected areas of which the listed area may be a nexus that is particularly critical for the listed function. Though it is common practice to refer to individual areas or groups as functional "centers" (eg, TO-1,2 as the "motion area") this can oversimplify the true connectional complexity, potentially leading to inappropriate clinical interpretation.

POS, postsubiculum; BMA, Bayesian model averaging; STS, superior temporal sulcus; EBA, extrastriate body area; ITS, inferior temporal sulcus; SFM, structure from motion; FFA, fusiform face area; WFA, word-form area; SFS, superior frontal sulcus; PCS, precentral sulcus; PPA, parahippocampal place area; IFS, inferior frontal sulcus; LIP, lateral intraparietal area; FEF, frontal eye field; DLPFC, dorsolateral prefrontal cortex.